Journal of Engineering Sciences, Assiut University, Vol. 40, No. 5, pp.1475-1486 - September 2012.

CHARACTERIZATION OF AL– AL_2O_3 NANOCOMPOSITE POWDERS SYNTHESIZED BY HIGH-ENERGY BALL MILLING

G. A. Abdalla[1], M. S. Aboraia[1], H. S. Wasly[2], M.A. Doheim[1], and A.E. Mahmoud[1]

[1] *Faculty of Engineering, Assiut University, Assiut*
[2] *Faculty of Engineering, Al-Azhar University, Qena*

(Received March 24, 2012 Accepted April 23, 2012)

Metal matrix composite powders of Al- Al2O3 with weight fraction of 20 % Al2O3 could be synthesized by high-energy milling of the mixed powders. Three different experiments were carried out at the same operating conditions, but with three different rotation speeds; 200, 300, and 400rpm. A homogenous distribution of the Al2O3 reinforcement in the Al matrix was obtained after milling the mixed powders for periods of 60, 45, and 30 h. The homogenous distribution of Al2O3 in the Al matrix was achieved by characterizing these nanocomposite powders by X-ray diffraction (XRD) and scanning electron microscopy (SEM) techniques. X-ray patterns were analyzed by using the Williamson–Hall treatment to determine the crystallite size and the lattice strain.

Keywords: *Al–Al2O3 metal matrix composites; High-energy milling; Nanostructure*

1. INTRODUCTION

Aluminum-based metal matrix composites (MMCs) are ideal materials for structural applications in the aircraft and automotive industries due to their light weight and high strength-to weight ratio [1-3]. Reinforcing the ductile aluminum matrix with stronger and stiffer second-phase reinforcements like ceramics provides a combination of properties of both the metallic matrix and the ceramic reinforcement components resulting in improved physical and mechanical properties of the composite [4,5]. Uniform dispersion of the fine reinforcements and a fine grain size of the matrix contribute to improving the mechanical properties of the composite. Further, the mechanical properties of the composite tend to improve with increasing volume fraction and decreasing particle size of the reinforcements [6-8].

The High energy ball milling technique is an effective method for producing powders for MMCs [9,10]. This process is achieved by repeated collisions of the grinding medium in the milling container made of hardened steel or tungsten carbide that the powder particles go through the repeated sequence of cold welding, fracturing, and rewelding. During each collision the powder particles get trapped between the colliding balls, between the ball and the inner surface of the vial and undergo severe plastic deformation [1]. A balance is achieved between the rate of welding that

increases the average composite particle size and the rate of fracturing that decreases the average composite particle size. This leads to a steady-state particle size distribution of the composite metal particles [1,11]. The continuous interaction between the fracture and welding events tends to refine the grain structure and leads to a uniform distribution of the fine reinforcement particles in the metal matrix [1].

The aim of the present work is to synthesize and characterize aluminum reinforced with a uniform dispersion of a specific weight fraction of alumina particles. The as-received micron size Al and Al_2O_3 powders are to be converted to a nanocomposite size by using the advanced powder metallurgy technique i.e., high-energy milling (HEM). The ceramic element, Al_2O_3, was chosen as the reinforcement, since it is chemically inert with Al and can also be used to higher temperatures, than the un-reinforced aluminum, with accompanying benefits of resistance to creep [1].

2. EXPERIMENTAL PROCEDURE

2.1 Materials

Commercial aluminum powder with a mesh size of -210 +90 μm was obtained from Elnasr Pharmaceutical Chemicals Company. Commercial alumina powder with particle size smaller than 44 μm was obtained from Egptalum Company. A mixture of Al-20 wt. % Al_2O_3 is used to investigate the effect of milling speed and milling time on the mechanical behavior of the composite material. A uniform distribution of the reinforcement phase and consolidation to full density are essential to achieve.

2.2 Milling of Powders

The powders were carefully mixed with the specific weight fraction of ceramic reinforcement (alumina). Planetary Monomill "Pulverisette 6" was used in the production of the composite powders, grinding employed under protective Argon gas. About 50 g of the powder mixture was loaded into the vial to maintain the 50 % free space. That's to obtain the optimum movement of balls and in turn transfer the milling energy to the mixture. The total weight of the hardened chrome steel balls was nearly close to 500 g. The ratio of ball-to-powder (BPR) is 10:1 and this ratio is maintained as indicated [1, 12] for better results. Three different rotation speeds of 200, 300, and 400 rpm are used in milling the powders.

The size of the balls also plays a critical role but in the present work balls of one size (20mm ϕ) are used. To minimize the sticking of the powders to the inner walls of the vial and the balls surface, about 5 wt. % of stearic acid was added as a process control agent (PCA). The duration of milling process is fixed by an electronic regulator on 30 min in order to avoid the temperature rise by milling. Samples were taken out at 7, 12, 15, 21, 30, 38, and 45 h for 300 rpm rotation speed, at 3, 7, 12, 15, 30, 38, 45 and 60h for the 200 rpm rotation speed, and at 3, 5, 7, 12, 15, 21, 27 and 30h for the 400 rpm rotation speed, to investigate the effect of milling time and rotation speed of mill, on homogeneity of Al_2O_3 distribution and particle size in the Al matrix as a nanocomposite material. It is worth noting that, for higher rotation speed of milling i.e, 300 and 400 rpm the experiment stopped as soon as the broadening in the x ray pattern has obtained i.e, 45 h and 30 h respectively.

2.3 Structural Analysis and Characterization

X-ray diffraction technique was used to identify the crystal structure and the phases present in the as-received and the milled composite powders. Distribution of Al_2O_3 particles in the Al matrix was checked with the aid of SEM imaging.

2.3.1 X-ray diffraction

X-ray diffraction (XRD) patterns were recorded for the as-received and milled powders with a Philips PW 1710 X-ray diffractometer using Cu Kα radiation (λ = 0.15406 nm) at 40 kV and 30mA settings. The XRD patterns were recorded in the 2 θ range of 20–80°. Comparison with standard XRD patterns enabled an unambiguous identification of the phases present in the milled powders [13].

During the powder milling process, the changes in peak shape are related to microstructural changes. The experimental line broadening is the result of three contributions, which are the crystallite size, lattice strains and the instrumental effects [14]. Several techniques, such as the Williamson–Hall [15] and Halder–Wagner methods [13], among others, are used to determine the grain size and the equivalent strain. The studies of the grain size refinement, identified on the basis of the microstructure and particle size studies, reported that plastic deformation, fracture and cold welding of powder particles were the three principle mechanisms which operate during mechanical milling [16-18].

In the Williamson–Hall treatment, the full width at half maximum (FWHM), β, due to sample imperfections is related to the crystallite size, *D*, and the distortions, ε, by the equation:

$$\beta^* = d^* \varepsilon + 1/D$$

where $\beta^* = \beta \cos\theta / \lambda$ and $d^* = 2 \sin\theta/\lambda$; θ is the Bragg angle and λ is the wavelength used. From the above equation, the intercept of the plot of β* against *d** gives 1/*D* and the slope gives the strain. The Williamson–Hall (WH) plot shows whether the breadth depends on *d** and the nature of any hkl planes dependence [19].

2.3.2 Scanning Electron Microscopy (SEM)

SEM images of the Al-Al_2O_3 composite powders were taken using JEOL-JSM 5400 LV scanning electron microscope. The equipment uses a cold cathode field emission source, has a resolution of 1.5 nm and a maximum magnification of 200,000X. Digital images can be captured using Link Isis oxford software that gives the flexibility of image control while still being able to adjust the contrast and brightness on the SEM. The main aim of the SEM analysis was to check the uniform distribution of alumina particles in the aluminum matrix.

3. RESULTS AND DISCUSSION

3.1 X-ray Diffraction Analysis

Figure 1 shows the X-ray diffraction patterns of the Al-Al_2O_3 powders milled with the three different rotation speeds; 200, 300, and 400 rpm. It can be seen, that line broadening increases with milling time. The main contributions to the decrease in

intensity and the broadening of the diffraction peaks are the grain size and the strain of the lattice, i.e., the reduction of crystallite size and lattice strain introduced by milling. From the direct examination of diffraction pattern during milling and comparison with standard XRD patterns of Al, Al_2O_3, obtained from ICDD (International Center for Diffraction Data) cards, it's noted that peak is shifted to high θ values. The creation of stacking faults by intensive deformation is probably one of the reasons of this shift [20]. The pattern decomposition analysis, using Williamson–Hall plot, showed an anisotropic broadening. This line profile analysis allows us to ascertain the evolution of the apparent size, D, and the equivalent lattice strain, ε, with milling time [21]. Figure 2 shows the variation of the crystallite size and of the lattice strain against milling time obtained by Williamson–Hall method, for Al-Al_2O_3 powders milled with 200, 300 and 400 rpm speed.

(a)

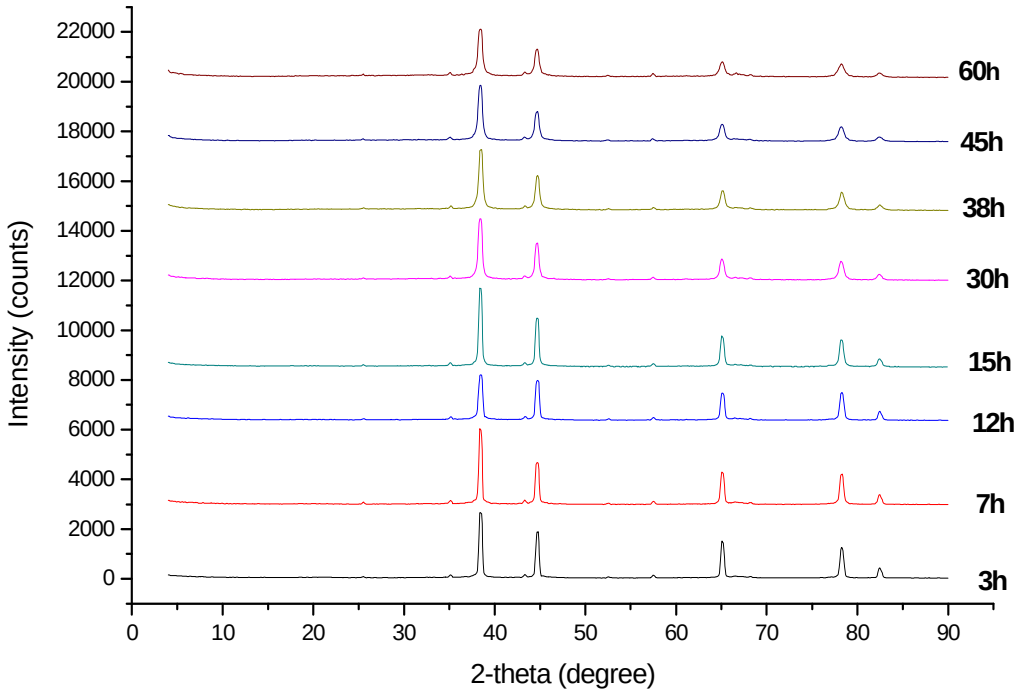

Fig. 1 : X-ray diffraction patterns of the Al–Al_2O_3 powders milled for different times (a) 200 rpm

(b)

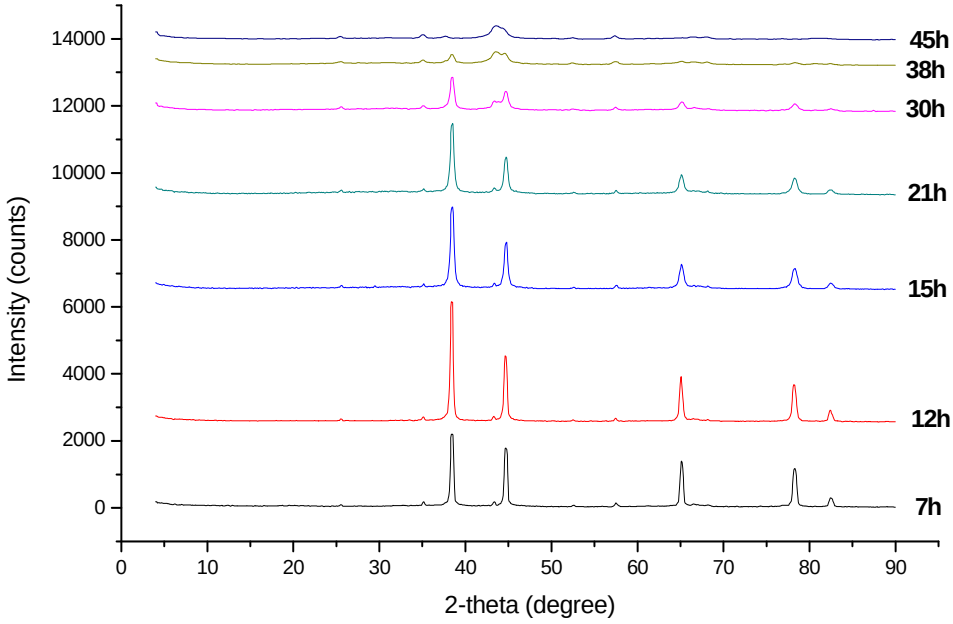

(c)

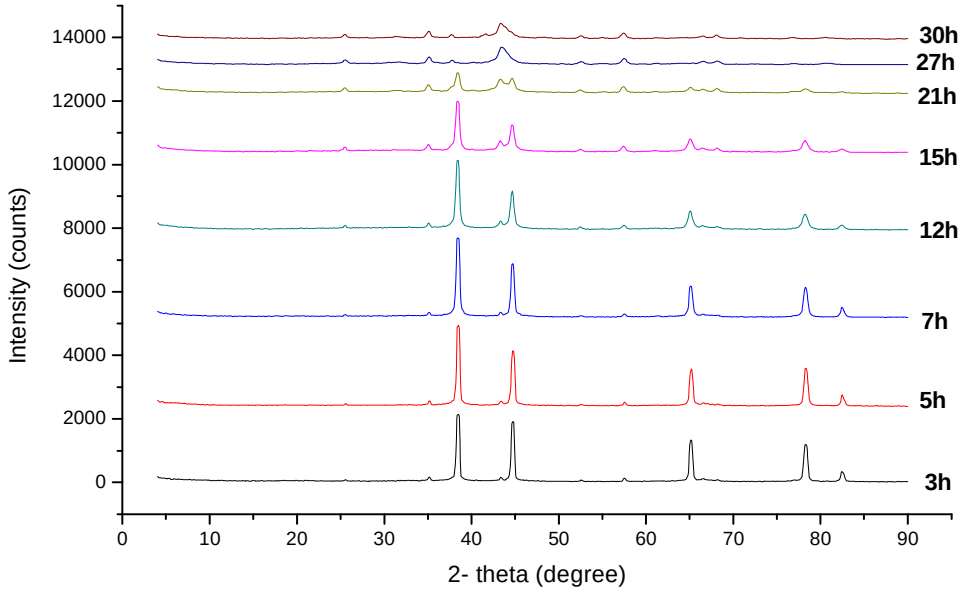

Fig. 1 (continue) : X-ray diffraction patterns of the Al–Al_2O_3 powders milled for different times (b) 300 rpm (c) 400 rpm.

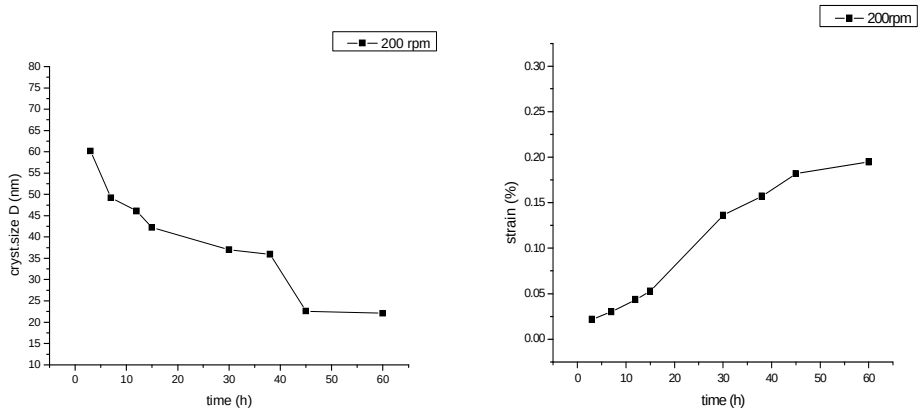

(a)

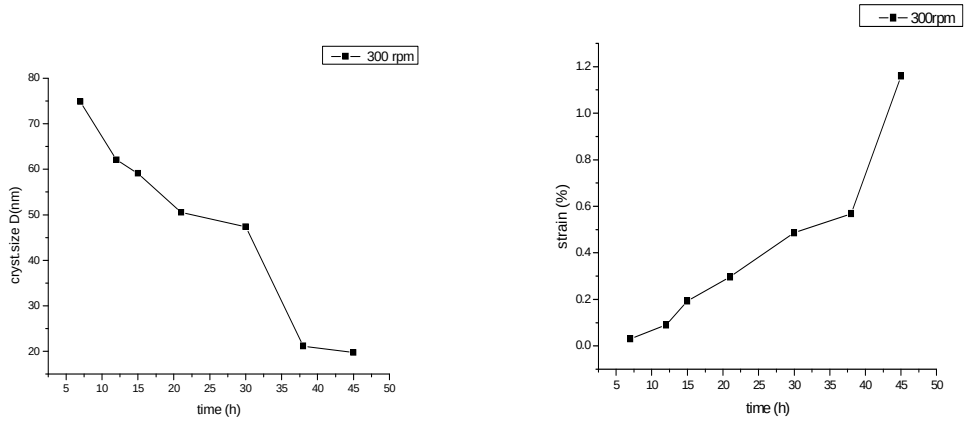

(b)

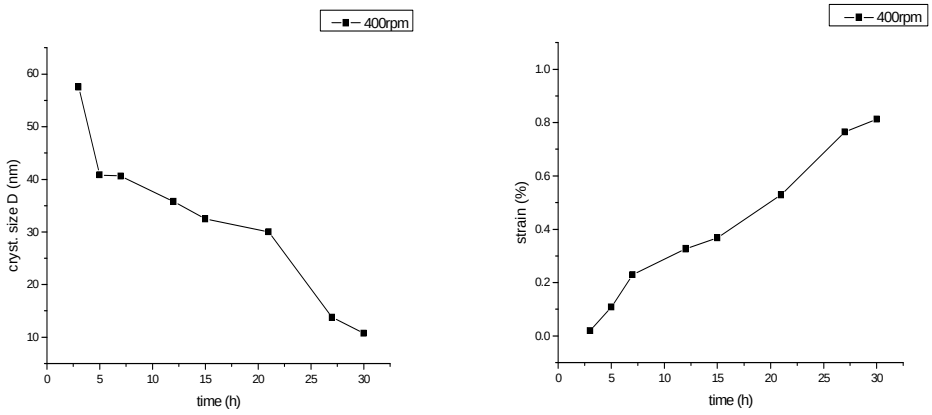

(c)

Fig.2 : Changes of crystallite size and lattice strain of the milled Al-Al_2O_3 powders as a function of milling time (a) 200 rpm (b) 300 rpm (c) 400 rpm.

It can be seen that the rate of the grain refinement continuously decreases reaching, after 60, 45, 30h of milling, the values of 22.1, 19.77 and 29.33 nm for Al-Al_2O_3 powders with 200, 300 and 400 rpm, respectively. On the other hand, the lattice strain shows a continuous increase to values of 0.20%, 1.16% and 0.81% (200, 300 and 400 rpm).

It is noted that the milling induces a higher lattice strain and an evolution of the finest particles, mainly in the extended times of milling. This behavior can be caused only by plastic deformation which will raise the lattice strain because of the increase of the defect density as well as dislocations of grain boundaries and lattice defects, in the initially relatively defect-free material. The influence of plastic deformation seems to disappear towards the extended milling, which can be concluded from the fact that the microstrains reach a saturation value, due to accumulated strain hardening of the powder material during plastic deformation [20].

3.2 Microstructural Observations

The major goal of the investigation was to ensure that a homogeneous distribution of Al_2O_3 in an aluminum matrix was achieved after milling. The reason behind this is the fact that a uniform distribution of reinforcement particles could potentially result in composites with improved mechanical properties. However, achieving this uniform distribution requires careful synthesis since clustering of the reinforcement particles would be a major constraint [1].

Figure 3 shows the SEM images of powder particles at different milling times at 300rpm. The powder particle size is changing with milling time, as a result of the two opposite actions of cold welding and fracturing. While cold welding increases the particle size, fracturing reduces the size [1]. At 0 hours milling time, Fig. 3(a), the agglomerated alumina particles are observed. This agglomeration can be removed by increasing the milling time. In the early stages of milling, Fig. 3(b), the particle distribution was not uniform and the distance between alumina particles was so high. Hence, with continued milling the powder particles size decreased due to the predominance of the fracturing of powder particles over the cold welding process. Once fracturing occurred, fresh particle surfaces are produced and due to the high reactivity of these surfaces, cold welding again becomes predominant leading to an Increase in particle size.

After 7h of milling the powder particles give flaky morphology. Also flaky morphology changed to equeiaxed morphology with increasing milling time to 30 h Fig. 3(c). At longer milling times (45 h) a balance is established between the cold welding and fracturing events and a steady-state situation is obtained. The powder particles were more uniform in size compared to the early stages of milling as shown in Fig. 3(d). The larger particles at longer milling times appeared to be an agglomeration of many smaller particles which was observed by others [22, 23].

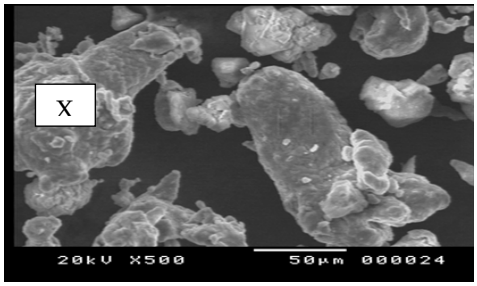

(a)

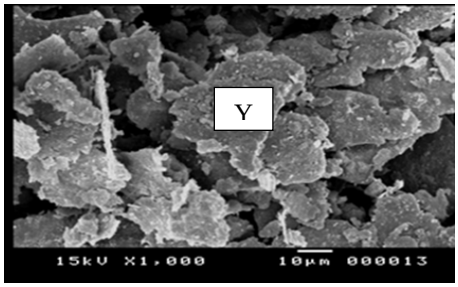

(b)

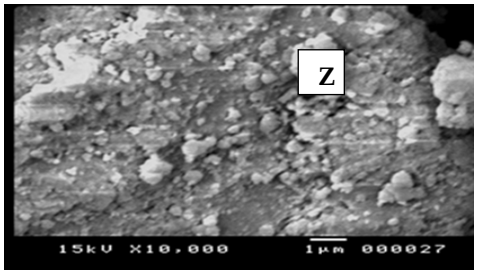

(c)

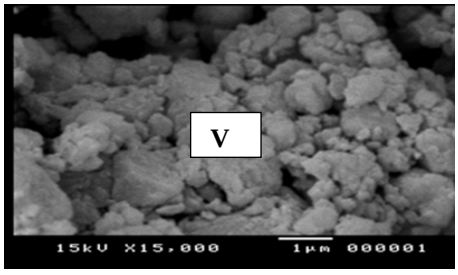

(d)

Fig. 3: SEM micrographs of Al–Al_2O_3 powders milled at 300 rpm after (a) 0 h, (b) 7 h, (c) 30 h, (d) 45h. ; X: agglomerations; Y: flattened particles ; Z: equeiaxed particles; V: Al_2O_3 uniform distribution after milling steady state (agglomerations for nanosize particles).

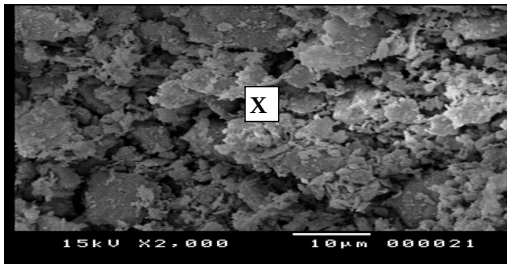

(a)

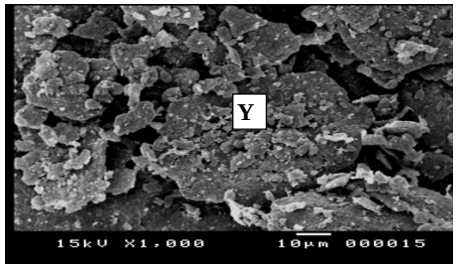

(b)

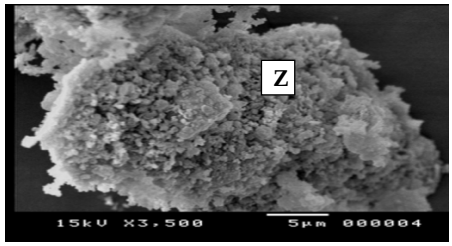

(c)

Fig. 4: SEM micrographs of Al–Al_2O_3 powders milled at 200rpm after (a) 7 h, (b) 30 h, (c) 45 h. ; X: flattened particles; Y: equeiaxed particles; Z: Al_2O_3 uniform distribution (agglomerations for nanosize particles).

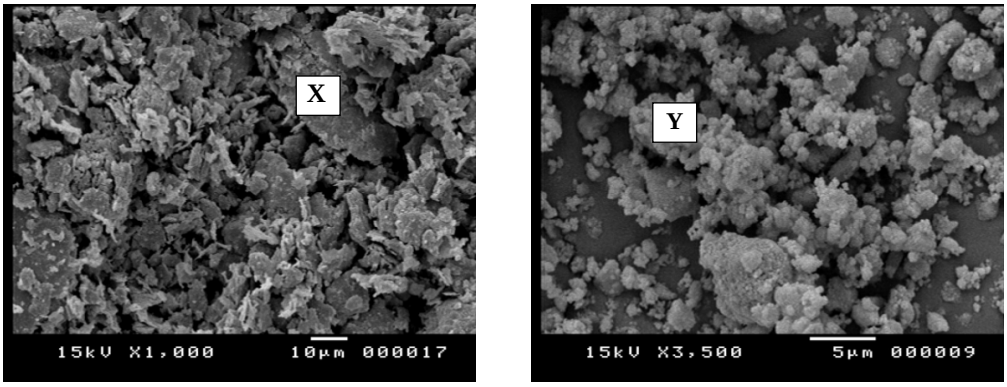

(a) **(b)**

Fig. 5: SEM micrographs of Al–Al_2O_3 powders milled at 400 rpm after (a) 7 h, (b) 30 h; X: flattened particles; Y: Al_2O_3 uniform distribution (agglomerations for nanosize particles)

The same state was found with the two other milling rotation speeds 200, 400 rpm in the milled powder mixtures. Instead of repeating similar observations for every milling rotation speed, only the final microstructures of the powders are shown in Figs. 4 & 5 for 200 and 400 rpm respectively.

A major concern in the present study is to investigate the nature and amount of impurities that contaminate the powder. The small size of the powder particles, availability of large surface area, and formation of new fresh surfaces during milling; all contribute to the contamination of the powder. Thus, it appears as though powder contamination is an inherent drawback of the technique, unless very special precautions are taken to avoid/minimize it [24]. Energy dispersive X-ray analysis (EDS) of the Al–Al_2O_3 mix without milling and the as-milled powders showed that the high-energy milling process introduce contamination into the milled powder. Fig. 6 shows the EDS spectra for the Al–Al_2O_3 mix without milling and the as-milled Al–Al_2O_3 powders milled at 300 rpm for 45 h. The presence of additional elements which are noticed from the peaks present in the as-milled Al–Al_2O_3 spectrum, confirmed that the milled powder contain elements (mainly iron) due to contamination from the milling media (grinding vessel and balls).

4. CONCLUSIONS

In the present study, nanosized powders of Al- Al_2O_3 have been synthesized by high energy ball milling. A uniform and homogenous distribution of the Al_2O_3 reinforcement in the Al matrix was obtained in the mechanically milled powder. By using WH method, it has shown that crystallite size decreases with milling time to steady values of 22.1, 19.77, 29.33 nm for rotation speeds 200, 300, 400rpm respectively. At the same time, the lattice strain increases to a steady values of 0.20%, 1.16% and 0.81% respectively.

(a)

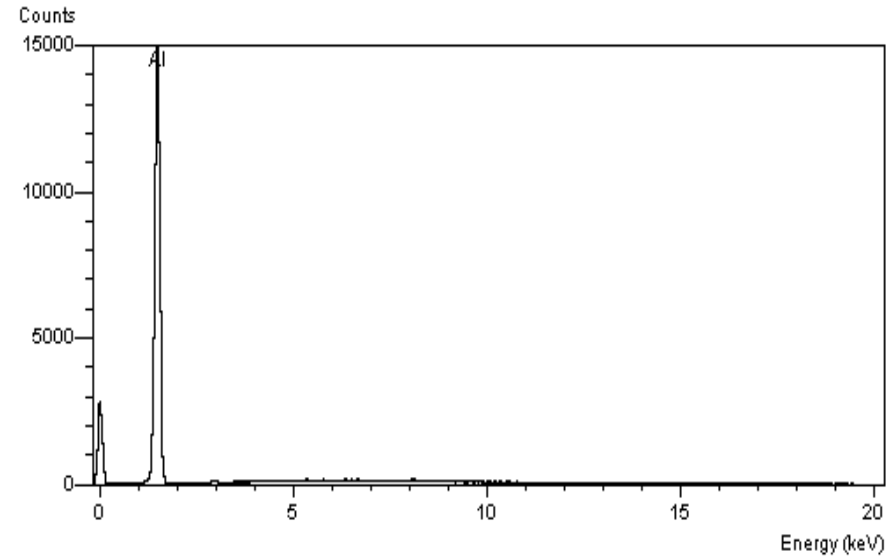

(b)

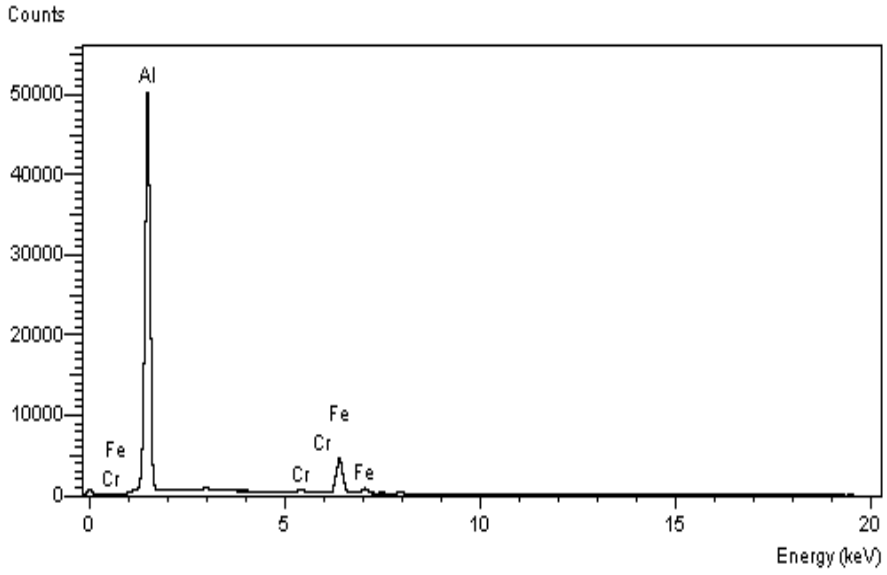

Fig. 6: EDS patterns of Al–Al_2O_3 powders milled at 300 rpm for 45 h: (a) Al-Al_2O_3 mix without milling, (b) as- milled Al–Al_2O_3 powders milled at 300 rpm for 45 h

REFERENCES

[1] B.Prabhu a, C. Suryanarayana, L. Ana, R. Vaidyanathan, Materials Science and Engineering A 425, (2006) 192–200.

[2] T.W. Clyne, P.J. Withers, An Introduction to Metal Matrix Composites, Cambridge Uni. press, UK, 1995.

[3] T. Graziani, A. Bellosi, D.D. Fabbriche, Int. J. Refr. Met Hard Mater. 11 (1992) 105–112.

[4] G.A. Cooper, A. Kelly, ASTM STP 452, Philadelphia, PA, 1969, ASTM.

[5] M.A. Piggott, Load Bearing Fiber Composites, Pergamon Press, London, 1980.

[6] W.J. Clegg, Acta Metall. 36 (1988) 2141–2149.

[7] C. Srinivasa Rao, G.S. Upadhyaya, Mater. Design 16 (1995) 359–366.

[8] T.J.A. Doel, P. Bowen, Composites A 27 (1996) 655–665.

[9] I.S. Polkin, A.B. Borzov, F.H. Froes. C. Suryanarayana, Proceedings of the Second International Conference on Structural Applications of Mechanical Alloying, Vancouver, Canada, 20-22 September, 1993, pp. 157-164.

[10] H.Zoz, H. Ren, Interceramics, 49, (1), (2000).

[11] J.S. Benajmin, T.E. Volin, Metall. Trans. 5 (1974) 1929–1934.

[12] K. W. Liu, F. Mucklich, Scripta Materialia, 49, (2003) 207- 212.

[13] C. Suryanarayana, M.G. Norton, X-ray Diffraction: A Practical Approach, Plenum, New York, 1998.

[14] J.I. Langford., J Appl. Crystallogr, 1978; 11:10–4.

[15] K.G.Williamson, H.W.Hall, Acta Metall 1953; 1:22.

[16] W. M. Kuschke, R. M. Keller, P. Grahle, R. Mason, and E. Arzt, Z. Metallkd.12, 804 (1995).

[17] J. Guerrero-paz, D.J. Vigueras, Nanostruct Mater 1999; 11: 1123–32.

[18] A.L.Salimon, A.M.Korsunsky, A.N.Ivanov, Mater Sci Eng 1999; A271:196–205.

[19] A. Rebhi,T. Makhlouf, N. Njah, Physics Procedia 2 (2009) 1263-1270.

[20] R. Daly, M.Khitouni, A.W. Kolsi, and N. Njah ,phys. stat. sol. (c) 3, No. 9, 3325–3331 (2006)/DOI 10.1002/pssc.200567112.

[21] M. Mhadhbi, M. Khitouni, M. Azabou, A. Kolsi, Materials Characterization 59, (2008) 944 – 950.

[22] H. Mahboob, S. A. Sajjadi, S. M. Zebarjad, the International Conference on MEMS and Nanotechnology, ICMN'08 13-15 May 2008, Kuala Lumpur Malaysia.

[23] Y.Mazaheri, F. Karimzadeh,M. H. Enayati , Materials Siences and Applications,2010,217-222.

[24] C. Suryanarayana, Prog. Mater. Sci. 46 (2001) 1–184.

توصيف مساحيق الألمونيوم – ألومينا النانونية والمنتجة باستخدام طاحونة كور عالية الطاقة

تم تكوين مسحوق متراكب من الألمونيوم والالومينا بحجم النانو بنسبة 20% الومينا وذلك باستخدام عملية الطحن عالية الطاقة 0 تم عمل ثلاث تجارب عند نفس الشروط ولكن تحت سرعات مختلفة للطاحونة وهي : 200، 400,300 لفة في الدقيقة ، تم الحصول علي توزيع متجانس للالومينا المقوية في خليط المساحيق بعد الطحن لمدد: 60، 45 ، 30 ساعة بالترتيب 0 وتم فحص المساحيق بواسطة أشعة اكس الحيودية والميكروسكوب الاليكتروني الماسح 0 وتم تحليل الصور والبيانات بواسطة طريقة (WH) لإيجاد حجم البلورات الدقيقة والإجهاد الواقع علي هيكل الشبكة البلورية .